

## Properties of Resonant Interatomic Coulombic Decay in Ne Dimers

T. Aoto,<sup>1</sup> K. Ito,<sup>1</sup> Y. Hikosaka,<sup>2</sup> E. Shigemasa,<sup>2</sup> F. Penent,<sup>3</sup> and P. Lablanquie<sup>2,3</sup>

<sup>1</sup>Photon Factory, Institute of Materials Structure Science, Oho, Tsukuba 305-0801, Japan

<sup>2</sup>UVSOR Facility, Institute for Molecular Science, Okazaki 444-8585, Japan

<sup>3</sup>LCP-MR, Université Pierre et Marie Curie-Paris 6 and CNRS (UMR 7614), 11 Rue Pierre et Marie Curie, 75231 Paris, France

(Received 27 July 2006; published 14 December 2006)

Properties of the interatomic Coulombic decay (ICD) process in Ne dimers have been obtained by tracking the formation of energetic Ne<sup>+</sup> ions. The double photoionization cross section, deduced from the Ne<sup>+</sup>/Ne<sup>+</sup> coincidence signal, is dominated by the ICD process and presents a threshold 280 meV below the atomic Ne<sup>+</sup>2s<sup>-1</sup> threshold. Rydberg excitation of a 2s electron in the dimer creates molecular Rydberg states whose Σ and Π symmetries have been resolved. These excited states decay by a resonant ICD process releasing an energetic Ne<sup>+</sup> ion and a neutral excited Ne\* fragment. Subsequent autoionization of the Ne\* fragment explains a double photoionization threshold below the dimer 2s ionization threshold.

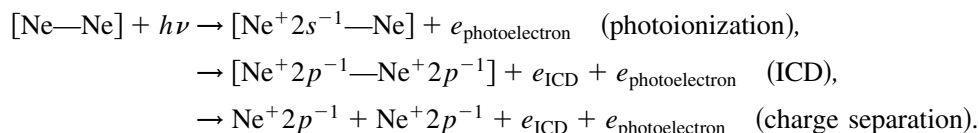
DOI: 10.1103/PhysRevLett.97.243401

PACS numbers: 36.40.-c, 33.20.Ni, 33.80.Eh, 34.30.+h

In rare gas atoms, inner-shell core holes can usually decay by emitting an Auger electron. This path is forbidden for inner-valence holes, as their binding energy lies below the lowest double ionization potential, and they can experience only a radiative decay. However, when the rare gas atom is part of a weakly bound van der Waals cluster, an alternative decay path is open whereby the initially ionized constituent atom transfers its energy to excite a neighboring atom. This process has been observed in Ar, Kr, and Xe dimers [1]. The energy transfer can sometime be sufficient to induce ionization. Such a new decay path was first predicted by Cederbaum *et al.* in H<sub>2</sub>O and HF clusters [2] and called interatomic or intermolecular Coulombic decay (ICD). ICD is predicted to be a general and very efficient decay mode for inner-valence holes, much faster than the competing intra-atomic decay. It has been predicted by theory in a variety of species, such as Ne

clusters [3–7], heteroatomic rare gas clusters [8], molecular clusters [2], or endohedral fullerenes [9]. ICD is also invoked to explain interatomic processes in Auger decays (SiF<sub>4</sub> [10] and xenon fluorides [11]).

Ne clusters have become model systems for ICD since the first theoretical prediction [3]. ICD was observed experimentally both in large Ne clusters [12–14] and in dimers [15]. Up to now, apart from Ne clusters, the only other system where an ICD process has been experimentally reported is the Ar cluster, after inner-shell ionization [16]. The ICD process in the Ne dimer can be schematically described in the following way: an inner-valence 2s electron is photoionized from a Ne atom inside the [Ne—Ne] dimer; the hole then decays by transferring its energy to the neighboring Ne atom and ejecting an outer valence 2p electron. As a result, a Ne dimer dication is created and decays by charge separation:



This localized description can be justified by the large internuclear separation in the ground state of the neutral Ne dimer and will be used for simplicity throughout this Letter. However, it has been shown [17] that the ICD mechanism is highly enhanced by the weak overlap between the orbitals of the two Ne units. In other words ICD can involve electrons from the van der Waals bond and a molecular description is often required.

In the present study, we bring new insight to bear on the ICD process for the Ne dimer by using an extremely simple experimental approach, namely, the observation of fast Ne<sup>+</sup> ions and Ne<sup>+</sup> ion pairs. This allows us to observe the whole 2s ionization channel in Ne dimers, to reveal the associated resonant ICD process, and to study its properties.

The experiment was performed at the undulator beam line BL-16B at the Photon Factory in Japan, equipped with a grazing incidence monochromator [18]. The photon resolution can be adjusted to between 4 and 20 meV. An aluminum filter is used to remove contamination by the second-order light of the monochromator. The photon energy is calibrated with atomic neon resonances lying below and above the Ne<sup>+</sup>2s<sup>-1</sup> threshold [19]. Ne dimers are produced by supersonic expansion through a 30 μm diameter nozzle at a stagnation pressure of 2.5 atm. The gas beam is unskipped and expands directly into the interaction region. The vacuum chamber is evacuated with a 20000 l/s cryopump. During measurements, the pressure in the chamber is maintained at about 3.0 × 10<sup>-5</sup> Torr. Under these conditions the particles present in the gas

beam are mainly Ne atoms with only a small fraction of dimers and almost no larger cluster. Two analyzers were used: a simple ion filter that rejects low energy or thermal ions and a hemispherical electrostatic analyzer equipped with position sensitive detection [20], which gives the kinetic energy distribution (KED) of energetic  $\text{Ne}^+$  ions. The hemispherical analyzer was operated at 40 eV pass energy, allowing a resolution of 200 meV (FWHM) and simultaneous detection over a range of ion kinetic energy from 0 to about 8 eV. The kinetic energy scale was calibrated by measuring the well known KED of  $\text{O}^+$  fragment ions resulting from the dissociation of the  $\text{O}_2^+(B^2\Sigma_g^-)$  and  $(c^4\Sigma_u^-)$  states [21]. The two analyzers faced one another to enable coincidence detection of the two  $\text{Ne}^+$  ions receding back to back and resulting from the ICD process. Contrary to Ref. [15], the dimer “ $2s$  photoelectron” is not simultaneously detected. This provides a higher coincidence efficiency and is, in principle, sensitive not only to ICD but also to all dissociative double ionization paths of the dimer.

The dimer double photoionization (DPI) cross section, as deduced from the  $\text{Ne}^+/\text{Ne}^+$  coincidence signal, is displayed in Fig. 1(c). Intense resonances are observed. A threshold in the vicinity of the  $2s$  atomic threshold demonstrates the link with the ICD process. Figure 2 shows three KED spectra of  $\text{Ne}^+$  ions detected in coincidence with a  $\text{Ne}^+$  partner. Two similar spectra are observed near the  $\text{Ne}^+2s^{-1}$  threshold, off and on resonance (photon energies of 48.50 and 48.84 eV, respectively). If we consider our somewhat lower resolution, they agree also with the results of Jahnke *et al.* [15] for  $\text{Ne}^+$  KED associated to the ICD process and with calculations [6]. These arguments suggest that the dimer double photoionization is largely dominated at threshold by the ICD process. This

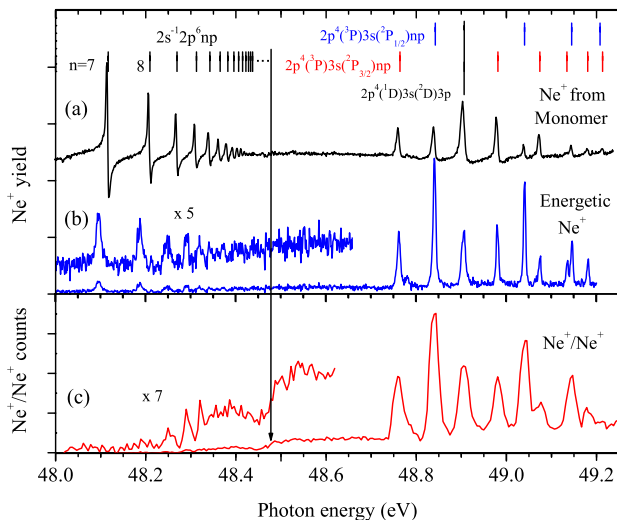


FIG. 1 (color online). (a) Yield of monomer  $\text{Ne}^+$  ions, detected in the hemispherical analyzer as having 0 eV kinetic energy, (b) yield of energetic ( $>1$  eV)  $\text{Ne}^+$  ions, detected by the ion filter, and (c) yield of  $\text{Ne}^+/\text{Ne}^+$  coincidences. Measurement was made at the magic angle.

is expected as ICD follows a one electron process (ionization of a  $2s$  electron) as opposed to the two electron process consisting in the simultaneous ejection of two  $2p$  electrons associated with different atoms constituent of the dimer. An additional structure appears on the high energy side of the KED peak measured at 58.80 eV. It was previously observed [22] but not in coincidence with the  $2s$  photoelectron [15], and is attributed to the ICD process following the formation of a  $\text{Ne} 2s$  satellite state inside the dimer. This additional structure is also weakly visible in the KED spectrum obtained at a photon energy of 53.10 eV (not shown), slightly above the  $\text{Ne}^+2p^4(^1D)3s$  satellite state at 52.1 eV [19,23], which suggests its origin in the ICD decay of excited Ne dimer states such as  $[\text{Ne}^+2p^43s-\text{Ne}]$ .

Yields of  $\text{Ne}^+$  ions from the monomer and of energetic  $\text{Ne}^+$  ions from the dimer are compared in Figs. 1(a) and 1(b). Energetic or fast ions are defined here as having more than 1 eV kinetic energy. Both yields have been simultaneously measured with a 4 meV photon resolution. A lower resolution of 20 meV was needed for the  $\text{Ne}^+/\text{Ne}^+$  coincidence measurement of Fig. 1(c). As discussed above, it can be viewed as the cross section for the  $\text{Ne} 2s$  ICD process, as long as the photon energy lies below the threshold of  $\text{Ne}^+ 2s$  satellite states. Above the  $\text{Ne}^+$  threshold, the  $\text{Ne}^+/\text{Ne}^+$  coincidence yield is found to be strictly proportional to the simultaneously measured yield of energetic  $\text{Ne}^+$  ions (not shown with 20 meV resolution). This suggests that all energetic ions are produced in pairs, as expected from the charge separation following the ICD process. The ICD cross section is found to be dominated by resonances above the atomic  $2s$  threshold. Their nature can be understood if we consider the yields of  $\text{Ne}^+$  ions from the monomer [Fig. 1(a)] and of energetic  $\text{Ne}^+$  ions from the dimers [Fig. 1(b)]. In the monomer, the resonances correspond to the  $2p^4(^3P)3s(^2P_{3/2,1/2})np$  Rydberg series strongly perturbed by the  $2p^4(^1D)3s(^2D)3p(^1P)$  resonance

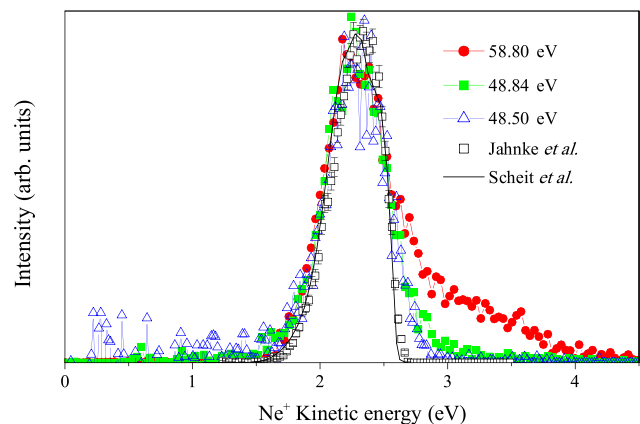
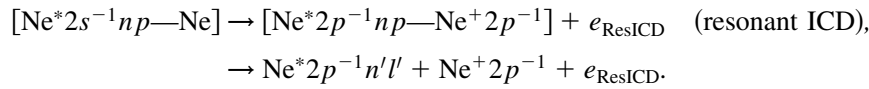


FIG. 2 (color online). Three KED spectra of  $\text{Ne}^+$  ions detected in coincidence with a  $\text{Ne}^+$  partner and obtained at the photon energy of 48.50, 48.84, and 58.80 eV. Solid black line: calculation by Scheit *et al.* [6]. Open squares: observation by Jahnke *et al.* [15].

[19]. Figure 1(b) shows that, in the dimer, resonances correspond to similar excitations of one Ne atom constituent of the dimer, that is to  $[\text{Ne}2p^43snp\text{---Ne}]$  excited states. Autoionization of such states into the dimer  $2s$  ionization channel  $[\text{Ne}^+2s^{-1}\text{---Ne}]$  is at the origin of the resonant character of the ICD process. The positions of resonances in the atom and in the dimer agree within experimental resolution, while their intensities and Fano profiles differ strongly. The reason is that the  $\text{Ne}^+$  yield from the atom [Fig. 1(a)] includes all  $2p$  and  $2s$  ionization continua, while the energetic  $\text{Ne}^+$  ion yield [Fig. 1(b)] specifically selects the inner-valence  $2s$  ionization channel in the dimer. Furthermore, the coupling of the resonances with the different ionization continua should differ in the atom and in the dimer.

The dimer DPI cross section [Fig. 1(c)] shows a threshold at 48.2 eV, some 280 meV below the atomic Ne  $2s$  threshold at 48.48 eV [19]. Some peaks and a broad band precede a step at the atomic Ne  $2s$  threshold. The ICD threshold is expected to occur at the  $2s$  ionization threshold in the dimer. However, calculations show that the lower  $[\text{Ne}^+2s^{-1}\text{---Ne}]$  ( $2^2\Sigma_u^+$ ) state presents a potential well of



Note that continuity of the energetic  $\text{Ne}^+$  signal at the  $2s$  threshold in Fig. 1(b) demonstrates a smooth transition between resonant ICD and ICD and suggests that for high  $[\text{Ne}2s^{-1}np\text{---Ne}]$  dimer Rydberg states the resonant ICD dominates, compared to the alternative autoionization paths to dimer ionic states. The  $\text{Ne}^*2p^{-1}n'l'$  fragment can be formed with a  $\text{Ne}^+2p^{-1}2P_{1/2}$  or  $2P_{3/2}$  core. For  $n'$

TABLE I. Properties of the dimer  $2s^{-1}np$  resonances. Energy shift (meV) gives the maximum position with respect to the atomic location [19]. FWHM (meV) is the observed full width at half maximum of the resonance. KE (eV) is the kinetic energy of the  $\text{Ne}^+$  fragment, measured at the magic angle.

$n$	$\Pi$ States		$\Sigma$ States		KE
	Energy shift	FWHM	Energy shift	FWHM	
4	-24	14	+14	38	1.5
5	-30	12.5	-13	15 <sup>a</sup>	1.7
6	-23	13 <sup>b</sup>	-17	10	1.9
7	-24	13 <sup>b</sup>	-19	12	2.0
8	-21	14 <sup>b</sup>	-21	12	2.1
9	-21	12 <sup>b</sup>	-21	13 <sup>b</sup>	2.2
10	-23	11 <sup>b</sup>	-23	13 <sup>b</sup>	c
11	-24	12 <sup>b</sup>	-23	12 <sup>b</sup>	c
12	-24	12 <sup>b</sup>	-25	12 <sup>b</sup>	c

<sup>a</sup>Two peaks are observed in the vicinity of the atomic  $2p^4(^3P)3s4p$  resonances [19].

<sup>b</sup>Asymmetric peak.

<sup>c</sup>KED of higher  $n$  Rydberg is observed to converge to the 2.3 eV ICD value (Fig. 2).

only 150 meV. Moreover, the ICD process cannot occur below the crossing between the potential curves of the  $\text{Ne}_2^+$  ( $2^2\Sigma_u^+$ ) state with the lower  $\text{Ne}_2^{++}$  one, predicted at 48.4 eV [6]. The 48.2 eV dimer DPI threshold must then have another origin than the simple ICD process.

Examination of energetic  $\text{Ne}^+$  ion yields in Fig. 1(b) gives us a clue: peaks are observed near the location of the atomic Ne  $2s^{-1}np$  resonances that give rise to Fano profiles in the  $\text{Ne}^+$  ion yield from the monomer [Fig. 1(a)]. Peaks are observed here as no other process produces energetic  $\text{Ne}^+$  ions off resonance, and interferences do not occur. The absence of similar peaks in the  $\text{Ne}^+/\text{Ne}^+$  coincidence signal suggests that these energetic  $\text{Ne}^+$  ions are formed with a neutral Ne partner. Values of the kinetic energy of these  $\text{Ne}^+$  ions formed on resonance are reported in Table I and are observed to converge at high  $n$  to the ICD value of Fig. 2. This leads us to suggest a resonant ICD process: photoexcitation of a  $2s$  electron in the dimer forms neutral  $[\text{Ne}2s^{-1}np\text{---Ne}]$  Rydberg states. Their core experiences ICD in the presence of the spectator  $np$  Rydberg electron, forming a  $[\text{Ne}2p^{-1}np\text{---Ne}^+2p^{-1}]$  ionic state that further dissociates according to

superior to around 13, depending on the  $l'$  value, the  $\text{Ne}^*2p^{-1}(^2P_{1/2})n'l'$  Rydberg can autoionize to the  $\text{Ne}^+2p^{-1}(^2P_{3/2})$  state [24]. This second step autoionization is proposed to be at the origin of the DPI coincidence signal below the  $2s$  threshold. As the  $\text{Ne}^*2p^{-1}(^2P_{3/2})n'l'$  Rydberg cannot autoionize, this explains also the observed step at the  $2s$  ionization threshold: resonant ICD ends up in single photoionization channel in this case, and this channel is closed at the  $2s$  threshold. Remarkably, double ionization is also present, though weak, down to  $n = 8$  Rydberg; this can arise if the  $np$  Rydberg electron does not remain a spectator during all the resonant ICD process and/or if the secondary electron is released in the dimer before full dissociation.

The term “resonant ICD” makes reference to the resonant Auger process. Resonant ICD was first detected by Barth *et al.* in large Ne clusters [14] following the  $\text{Ne}2s \rightarrow 3p$  excitation, and a theoretical model was recently developed and applied to the  $\text{MgNe}$  cluster [25]. The present experiment brings to light details of the resonant ICD in Ne dimers. Information on the molecular  $[\text{Ne}2s^{-1}np\text{---Ne}]$  Rydberg states is given by high resolution angular resolved ion yields in Fig. 3. As their lifetime is expected to be comparable to the fast ICD one, which is predicted to be around 80 fs in the dimer [7], the axial recoil approximation holds and fragments are expected to reflect orientation of the molecular axis upon photon absorption.  $\Sigma$  and  $\Pi$  symmetries are obtained from ions emitted at  $0^\circ$  and  $90^\circ$  with respect to the electric vector of the linearly polarized light, as reported in Fig. 3. Peak shifts with respect to the

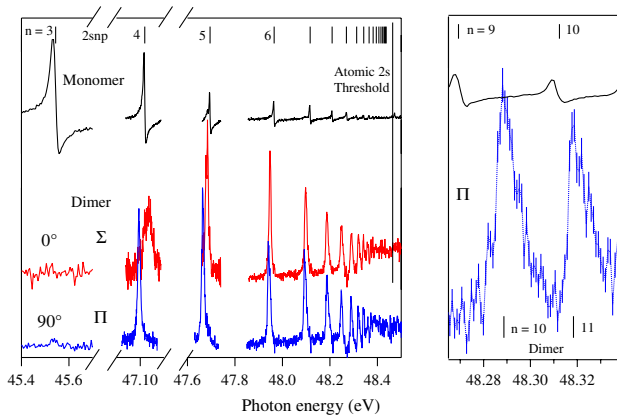


FIG. 3 (color online). Angle resolved yields of energetic  $\text{Ne}^+$  ions, compared to ion yield from the monomer (top). The center and bottom lines correspond, respectively, to the energetic  $\text{Ne}^+$  emitted at  $0^\circ$  and  $90^\circ$  with respect to the light polarization. They trace states of  $\Sigma$  and  $\Pi$  symmetry. Photon resolution was set at 4 meV.

atomic  $\text{Ne}^* 2s^{-1}np$  resonances are clearly observed. While at high  $n$  values  $\Sigma$  and  $\Pi$  contributions are very similar, they differ markedly for the  $n = 4$  and  $5$  levels. The broad  $n = 4$   $\Sigma$  resonance is atypical and could reflect a possible valence character or some steric hindrance, due to the fact that for  $n = 4$  the Rydberg orbital is roughly of the same size as the dimer. The absence of the  $n = 3$  resonance in the dimer could be due to a large shift with respect to the atomic position, as predicted in the  $\text{MgNe}$  system. It could also be attributed to a dominant autoionization path [25], and indeed autoionization may be at the origin of the lower intensity of the  $n = 4$  peaks compared to the  $n = 5$  ones. Except for the broad  $n = 4$  resonance, all peaks are narrow, with a width in excess of the 4 meV photon resolution and of the order of 12 meV. Asymmetry of the peaks is also observed, with a sharper low energy edge (see enlarged  $n = 10$  and  $11$  peaks in Fig. 3). Surprisingly, the maximum of all high  $n$  Rydbergs is located some 24 meV below their atomic counterpart. If we consider that high Rydbergs reflect the properties of the ionic core they converge to, this suggests a convergence to a vibrational level bound by that energy amount (minus the binding energy of the  $v = 0$  level of the ground  $\text{Ne}_2$  state). Calculations [4,5] suggest it is the  $2^2\Sigma_u^+$  eighth vibrational state. The high energy tail is believed to reflect the contribution of unresolved higher vibrational levels of the  $2^2\Sigma_u^+$  state and possibly of the only predicted  $2^2\Sigma_g^+$  vibrational level. Furthermore, the lifetime broadening of the Rydberg levels can contribute to their observed width. Measurements with a higher photon resolution might give estimates for the ICD lifetime.

ICD has recently attracted much interest as a process by which energy can be transferred from a given center to its environment. It is believed to have important consequences for chemistry, solid state physics, and biology [15,16]. The present work brings important basic information on the process, thanks to the simple experimental method to ob-

serve energetic  $\text{Ne}^+$  ions from  $\text{Ne}$  dimers with or without coincidence: double photoionization is dominated by the ICD process and traces its cross section, which shows strong resonances due to double excitation of one  $\text{Ne}$  unit. Rydberg excitation of a  $2s$  electron creates molecular Rydbergs of the  $[\text{Ne}2s^{-1}np-\text{Ne}]$  type, which are observed to decay by a resonant ICD process, producing energetic  $\text{Ne}^+$  ions. Symmetries of these states were separated. Secondary autoionization of the  $\text{Ne}^*$  fragment released in the resonant ICD process is proposed to explain the DPI threshold observed some 280 meV below the  $2s$  atomic threshold. It is expected that this experimental method will bring new insight on ICD processes in other systems. Work is in progress on other rare gas dimers [26].

The present work was performed under the approval of the Photon Factory (PF) Advisory Committee (Proposal No. 2004G010). The authors are indebted to L. Cederbaum and S. Scheit for fruitful discussions and would like to thank C. Hague for a critical reading of the manuscript and the PF staff for the support during the beam time.

- 
- [1] R. Thissen *et al.*, Eur. Phys. J. D **4**, 335 (1998).
  - [2] L. S. Cederbaum, J. Zobeley, and F. Tarantelli, Phys. Rev. Lett. **79**, 4778 (1997).
  - [3] R. Santra *et al.*, Phys. Rev. Lett. **85**, 4490 (2000).
  - [4] N. Moiseyev *et al.*, J. Chem. Phys. **114**, 7351 (2001).
  - [5] S. Scheit, L. S. Cederbaum, and H.-D. Meyer, J. Chem. Phys. **118**, 2092 (2003).
  - [6] S. Scheit *et al.*, J. Chem. Phys. **121**, 8393 (2004).
  - [7] R. Santra, J. Zobeley, and L. S. Cederbaum, Phys. Rev. B **64**, 245104 (2001).
  - [8] S. Scheit *et al.*, J. Chem. Phys. **124**, 154305 (2006).
  - [9] V. Averbukh and L. S. Cederbaum, Phys. Rev. Lett. **96**, 053401 (2006).
  - [10] T. D. Thomas *et al.*, Phys. Rev. Lett. **89**, 223001 (2002).
  - [11] C. Buth, R. Santra, and L. S. Cederbaum, J. Chem. Phys. **119**, 10 575 (2003).
  - [12] S. Marburger *et al.*, Phys. Rev. Lett. **90**, 203401 (2003).
  - [13] G. Öhrwall *et al.*, Phys. Rev. Lett. **93**, 173401 (2004).
  - [14] S. Barth *et al.*, J. Chem. Phys. **122**, 241102 (2005).
  - [15] T. Jahnke *et al.*, Phys. Rev. Lett. **93**, 163401 (2004).
  - [16] Y. Morishita *et al.*, Phys. Rev. Lett. **96**, 243402 (2006).
  - [17] V. Averbukh, I. B. Müller, and L. S. Cederbaum, Phys. Rev. Lett. **93**, 263002 (2004).
  - [18] E. Shigemasa *et al.*, J. Synchrotron Radiat. **5**, 777 (1998).
  - [19] K. Schulz *et al.*, Phys. Rev. A **54**, 3095 (1996).
  - [20] Y. Hikosaka *et al.*, Meas. Sci. Technol. **11**, 1697 (2000).
  - [21] Y. Hikosaka *et al.*, J. Phys. B **36**, 1423 (2003).
  - [22] T. Jahnke, Ph.D. thesis, Frankfurt University, 2005.
  - [23] A. Kikas *et al.*, J. Electron Spectrosc. Relat. Phenom. **77**, 241 (1996).
  - [24] V. Kaufman and L. Minnhagen, J. Opt. Soc. Am. **62**, 92 (1972).
  - [25] K. Gokhberg, V. Averbukh, and L. S. Cederbaum, J. Chem. Phys. **124**, 144315 (2006).
  - [26] P. Lablanquie, T. Aoto, Y. Hikosaka, F. Penent, Y. Morioka, and K. Ito (to be published).